Electronic Supplementary Information

Experimental section

Materials: Ethanol was purchased from Aladdin Ltd. (Shanghai, China). $La(NO_3)_3·6H_2O$, $Ti(SO_4)_2$, La_2O_3, TiO_2, NaOH, Sulfuric acid (H_2SO_4), hydrochloric acid (HCl), aniline, ammonium chloride (NH_4Cl), hydrazine hydrate ($N_2H_4·H_2O$), dimethylaminobenzaldehyde ($C_9H_{11}NO$), sodium citrate dehydrate ($C_6H_5Na_3O_7·2H_2O$), sodium nitroferricyanide dihydrate ($C_5FeN_6Na_2O·2H_2O$), sodium hydroxide (NaOH), and sodium hypochlorite solution (NaClO) were purchased from Beijing Chemical Corp. (China). Nafion (5 wt%) was purchased from Sigma-Aldrich Chemical Reagent Co. Ltd. All reagents were analytical reagent grades and used as received without further purification. The water in this study was purified through a Millipore system.

Preparation $La_2Ti_2O_7$: $La_2Ti_2O_7$ (LTO) nanosheet was obtained by facile hydrothermal method. 2 mmol of $La(NO_3)_3·6H_2O$ and 2 mmol of $Ti(SO_4)_2$ were added into 10 mL water under sonication. After that, 10 ml NaOH aqueous solution (2 M) was dropped into the above solution. After magnetically stirring for 4 h, the mixture was transferred into a teflon autoclave (50 mL) and then heated at 240 °C for 24 h. After reaction, the autoclave cooled to room temperature naturally. The white precipitates were collected by high-speed centrifugation, and washed with water, hydrochloric acid, and ethanol thoroughly. The products were dried in air at 80 °C for overnight. Bulk LTO was synthesized by a solid-reaction between reagent grade La_2O_3 and TiO_2 powder, which were mixed with a mole ratio of 1:2. The mixture was wet ground in ethanol solution for 3 h. The ground wet powder was then dried in an oven at 100 °C K for 24 h and sintered at different temperatures between 1100 °C for15 h.

Preparation of LTO-CP electrode: 10 mg LTO powders and 40 μL of Nafion solution (5 wt%) were dispersed in 960 μL mixed solution contains 480 μL ethanol and 480 μL H_2O by 2 h sonication to form a homogeneous ink. Then, 10 μL LTO was loaded on a CP with area of 1 x 1 cm^2 and dried under ambient condition.

Characterization: XRD patterns were obtained from a Shimazu XRD-6100 diffractometer with Cu Kα radiation (40 kV, 30 mA) of wavelength 0.154 nm (Japan). TEM images were obtained from a Zeiss Libra 200FE transmission electron microscope operated at 200 kV. The X-ray photoelectron spectroscopy (XPS) measurements were performed on an ESCALABMK II X-ray photoelectron spectrometer using Mg as the exciting source. The absorbance data of spectrophotometer were measured on SHIMADZU UV-1800 ultraviolet-visible (UV-Vis) spectrophotometer. SEM images were collected from the tungsten lamp-equipped SU3500 scanning electron microscope at an accelerating voltage of 20 kV (HITACHI, Japan).

Electrocatalytic measurements: N_2 reduction reaction (NRR) experiments were carried out in a two-compartment cell under ambient condition, which was separated by the Nafion 117 membrane. The membrane was protonated by first boiling in ultrapure water for 1 h and treating in H_2O_2 (5%) aqueous solution at 80 °C for another 1 h, respectively. The membrane was then treated in 0.5 M H_2SO_4 for 3 h at 80 °C and finally in water for 6 h. All experiments were carried out at room temperature. The electrochemical experiments were carried out with an electrochemical workstation (CHI 660E) using a three-electrode configuration including prepared electrodes, graphite rod and Ag/AgCl electrode (saturated KCl solution) serving as the working electrode, counter electrode and reference electrode, respectively. The potentials reported in this work were converted to reversible hydrogen electrode (RHE) scale via calibration with the following equation: $E \text{ (vs. RHE)} = E \text{ (vs. Ag/AgCl)} + 0.059 \times \text{pH} + 0.197$ V and the presented current density was normalized to the geometric surface area. For electrochemical NRR, chrono-amperometry tests were conducted in N_2-saturated 0.1 M HCl solution.

Determination of NH_3: Concentration of produced NH_3 was spectrophotometrically determined by the indophenol blue method.[1] Typically, 2 mL HCl electrolyte was taken from the cathodic chamber, and then 2 mL of 1 M NaOH solution containing 5% salicylic acid and 5% sodium citrate was added into this solution. Subsequently, 1 mL of 0.05 M NaClO and 0.2 mL of 1% $C_5FeN_6Na_2O\cdot 2H_2O$ were add into the above solution. After standing at room temperature for 2 h, the UV-Vis absorption absorption spectrum was measured at a wavelength of 655 nm. The concentration-absorbance curves were calibrated using standard NH_4Cl solution with a serious of concentrations. The fitting curve ($y = 0.427x + 0.067$, $R^2 = 0.999$) shows good linear relation of absorbance value with NH_4Cl concentration by three times independent calibrations.

Determination of N_2H_4: The N_2H_4 in the electrolyte was estimated by the method of Watt and Chrisp.[2] A mixture of p-$C_9H_{11}NO$ (5.99 g), HCI (concentrated, 30 mL) and C_2H_5OH (300 mL) was used as a color reagent. In detail, 5 mL electrolyte was removed from the electrochemical reaction vessel, and added into 5 mL above prepared color reagent and stirring 10 min at room temperature. The absorbance of the resulting solution was measured at 455 nm. Absolute calibration of this method was carried out using the $N_2H_4\cdot H_2O$ solution as a standard, and the fitting curve showed a good linear relation of absorbance with the $N_2H_4\cdot H_2O$ concentration ($y= 0.511x + 0.0364$, $R^2 = 0.999$).

Calculations of NH_3 yield and FE: NH_3 yield was calculated using the following equation:

$$NH_3 \text{ yield} = [NH_3] \times V / (t \times m_{cat.})$$

FE was calculated according to following equation:

$$FE = 3 \times F \times [NH_3] \times V / (17 \times Q)$$

where $[NH_3]$ is the measured NH_3 concentration; V is the volume of the cathodic reaction electrolyte; t is the potential applied time; $m_{cat.}$ is the loaded quality of catalyst; F is the Faraday constant and Q is the quantity of charge in Coulombs.

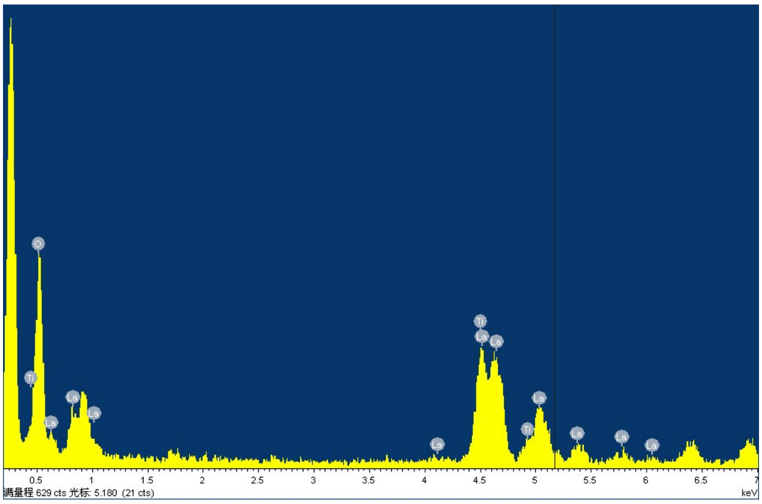
O
Ti
La
0.5
1
1.5
2
2.5
3
3.5
4
4.5
5
5.5
6
6.5
7
keV
满量程 629 cts 光标: 5.180 (21 cts)

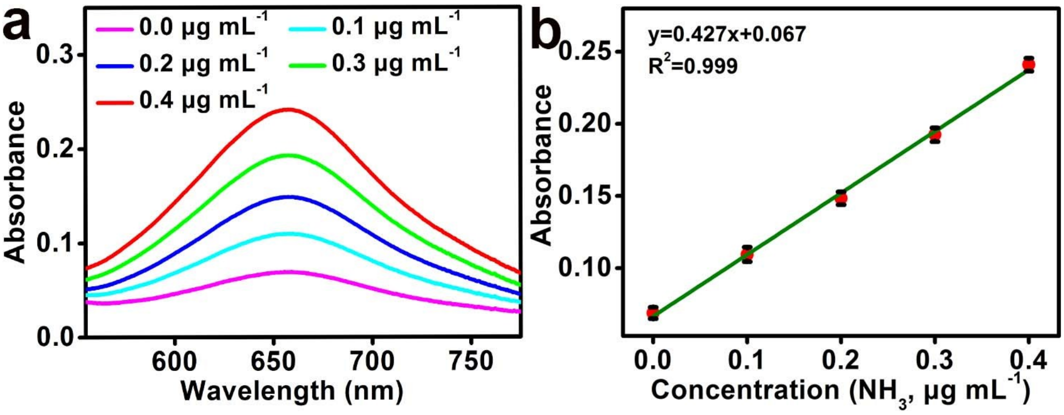
a
0.0 μg mL-1
0.1 μg mL-1
0.2 μg mL-1
0.3 μg mL-1
0.4 μg mL-1
Absorbance
Wavelength (nm)
0.0
0.1
0.2
0.3
600
650
700
750
b
y=0.427x+0.067
R2=0.999
Absorbance
Concentration (NH3, μg mL-1)
0.10
0.15
0.20
0.25
0.0
0.1
0.2
0.3
0.4

Fig. S2. (a) UV-Vis absorption spectra of various NH_3 concentrations after incubation for 2 h at room temperature. (b) Calibration curve used for calculation of NH_3 concentrations by three times independent calibrations.

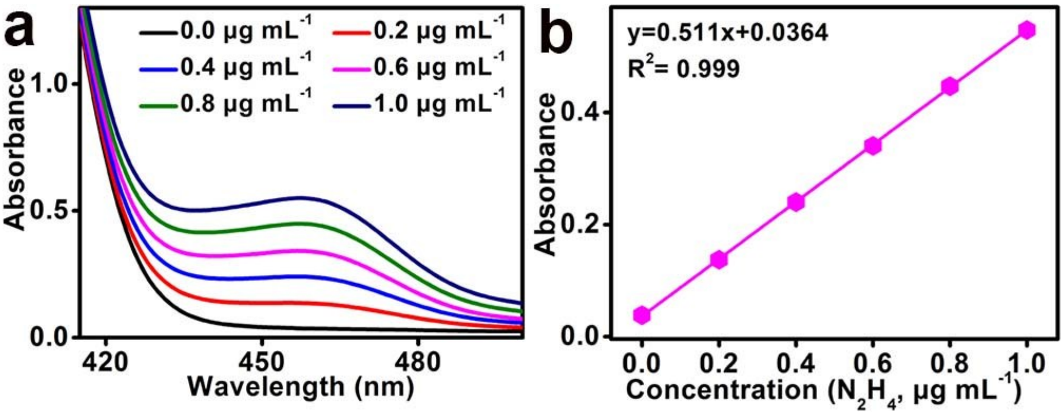

Fig. S3. (a) UV-Vis absorption spectra of various N_2H_4 concentrations after incubation for 10 min at room temperature. (b) Calibration curve used for calculation of N_2H_4 concentrations.

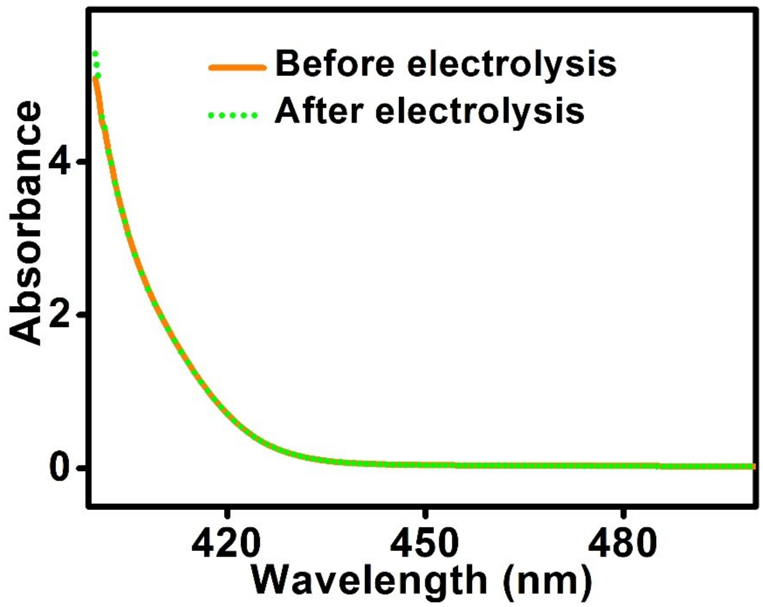

Fig. S4. UV-Vis absorption spectra of the electrolytes estimated by the method of Watt and Chrisp before and after 2 h electrolysis in N_2 atmosphere at –0.55 V using LTO-CP as the working electrode.

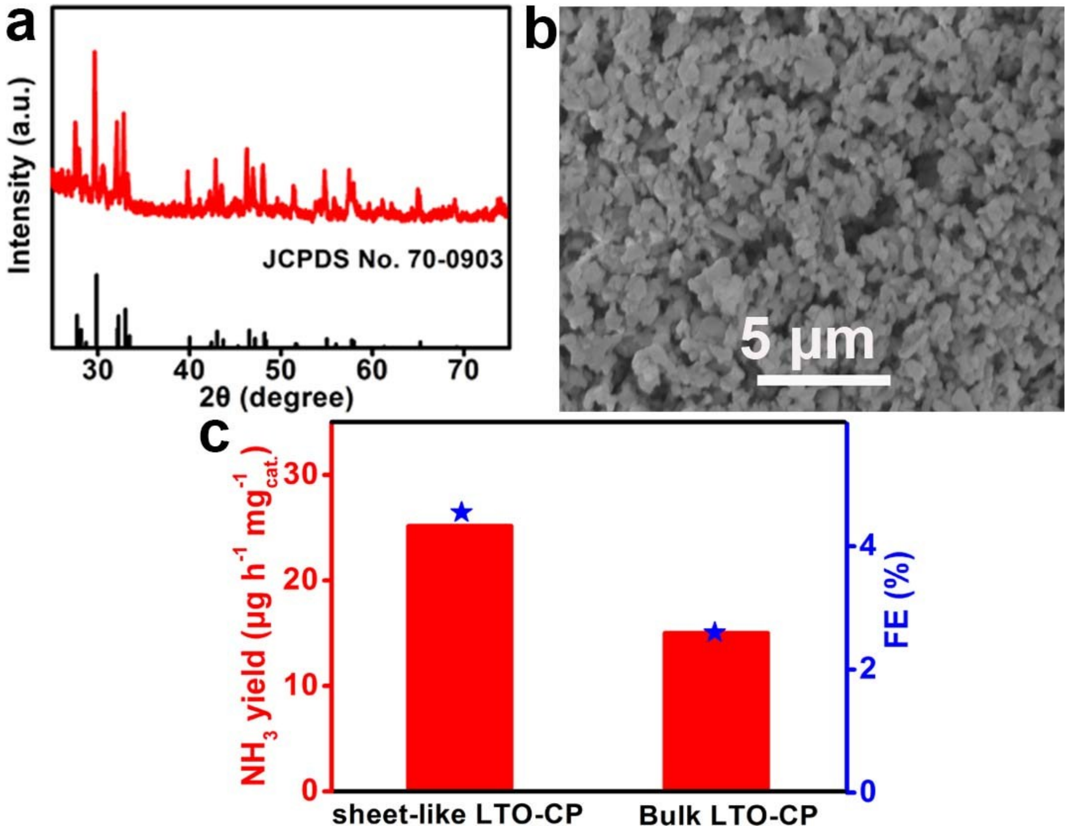

Fig. S5. (a) XRD patten and (b) SEM image for bulk LTO. (c) NH_3 yields and FEs for sheet-like LTO-CP and bulk LTO-CP at –0.55 V after 2 h electrolysis in 0.1 M HCl.

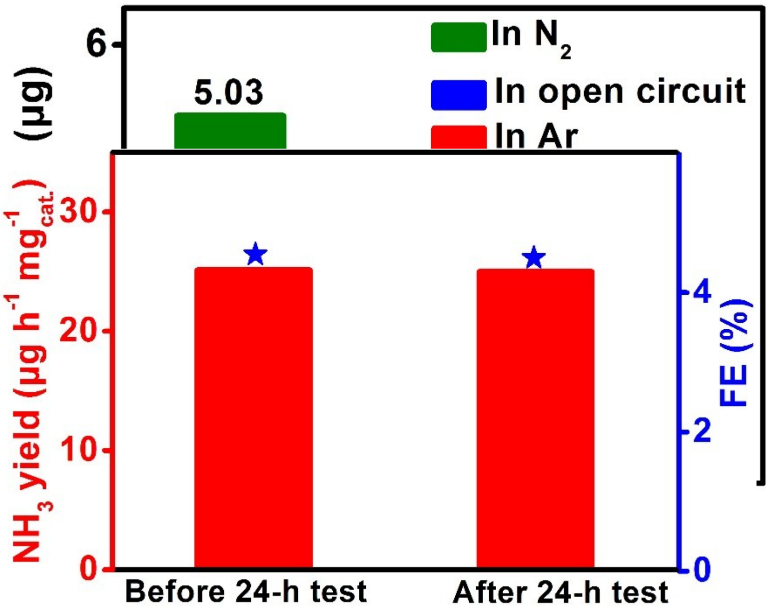

Fig. S6. NH_3 produced with LTO-CP at –0.55 V after 2 h electrolysis under different conditions.

Fig. S7. NH_3 yields and FEs of LTO-CP before and after 24-h test at –0.55 V.

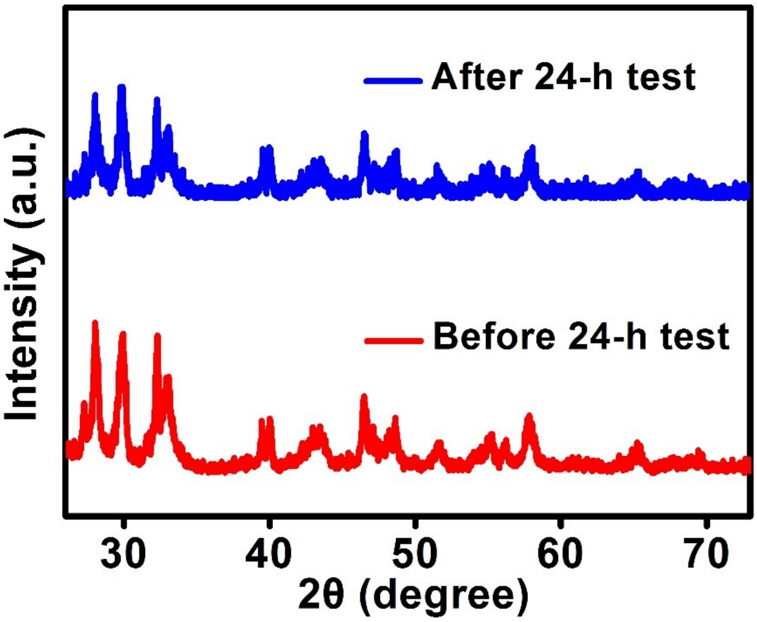

Fig. S8. XRD patterns for LTO before and after 24-h test.

Table S1. Comparison of the electrocatalytic N_2 reduction performance for LTO-CP with other aqueous-based NRR electrocatalysts.

Catalyst	**Electrolyte**	**NH_3 yield rate**	**FE (%)**	**Ref.**
LTO-CP	**0.1 M HCl**	**22.5 μg h^{-1} $mg^{-1}_{cat.}$**	**4.1**	**This work**
VN	0.1 M HCl	9.55 μg h^{-1} $mg^{-1}_{cat.}$	3.58	3
NPC	0.1 M HCl	15.7 μg h^{-1} $mg^{-1}_{cat.}$	1.45	4
Ag nanosheet	0.1 M HCl	4.62×10^{-11} mol s^{-1} cm^{-2}	4.8	5
MoN	0.1 M HCl	3.01×10^{-10} mol s^{-1} cm^{-2}	1.15	6
Mo nanofilm	0.01 M H_2SO_4	3.09×10^{-11} mol s^{-1} cm^{-2}	0.72	7
PEBCD/C	0.5 M Li_2SO_4	1.58 μg h^{-1} cm^{-2}	2.85	8
Mn_3O_4 nanocube	0.1 M H_2SO_4	11.6 μg h^{-1} $mg^{-1}_{cat.}$	3.0	9
TiO_2-rGO	0.1 M Na_2SO_4	15.13 μg h^{-1} $mg^{-1}_{cat.}$	3.3	10
Fe_2O_3 nanorods	0.1 M Na_2SO_4	15.9 μg h^{-1} $mg^{-1}_{cat.}$	0.94	11
γ-Fe_2O_3	0.1 M KOH	0.212 μg h^{-1} $mg^{-1}_{cat.}$	1.9	12
Au nanorods	0.1 M KOH	6.04 μg h^{-1} mg^{-1} cat.	4	13
Ru/C	2 M KOH	0.21 μg h^{-1} cm^{-2}	0.28	14
MoS_2	0.1 M Na_2SO_4	0.02 μg h^{-1} cm^{-2}	1.17	15
Fe_2O_3-CNT	$KHCO_3$	0.22 μg h^{-1} cm^{-2}	0.15	16
oxygen-doped carbon nanosheet	0.1 M HCl	20.15 μg h^{-1} $mg^{-1}_{cat.}$	4.97	17
$Bi_4V_2O_{11}/CeO_2$	0.1 M HCl	23.21 μg h^{-1} mg^{-1} cat.	10.16	18
N-doped nanocarbon	0.05 M H_2SO_4	27.20 μg h^{-1} mg^{-1} cat.	1.42	19
polymeric carbon nitride	0.1 M HCl	8.09 μg h^{-1} $mg^{-1}_{cat.}$	11.59	20
hollow Cr_2O_3 microspheres	0.1 M Na_2SO_4	25.3 μg h^{-1} $mg^{-1}_{cat.}$	6.78	21

References

1 D. Zhu, L. Zhang, R. E. Ruther and R. J. Hamers, *Nat. Mater.*, 2013, **12**, 836–841.

2 G. W. Watt and J. D. Chrisp, *Anal. Chem.*, 1952, **24**, 2006–2008.

3 X. Zhang, R. Kong, H. Du, L. Xia and F. Qu, *Chem. Commun.*, 2018, **54**, 5323–5325.

4 X. Yang, K. Li, D. Cheng, W. Pang, J. Lv, X. Chen, H. Zang, X. Wu, H. Tan, Y. Wang and Y. Li, *J. Mater. Chem. A*, 2018, **6**, 7762–7769.

5 H. Huang, L. Xia, X. Shi, A. M. Asiri and X. Sun, *Chem. Commun.*, 2018, **54**, 11427–11430.

6 L. Zhang, X. Ji, X. Ren, Y. Luo, X. Shi, A. M. Asiri, B. Zheng and X. Sun, *ACS Sustainable Chem. Eng.*, 2018, **6**, 9550–9554.

7 D. Yang, T. Chen and Z. Wang, *J. Mater. Chem. A*, 2017, **5**, 18967–18971.

8 G. Chen, X. Cao, S. Wu, X. Zeng, L. Ding, M. Zhu and H. Wang, *J. Am. Chem. Soc.*, 2017, **139**, 9771–9774.

9 X. Wu, L. Xia, Y. Wang, W. Lu, Q. Liu, X. Shi and X. Sun, *Small*, 2018, **14**, 1803111.

10 X. Zhang, Q. Liu, X. Shi, A. M. Asiri, Y. Luo, X. Sun and T. Li, *J. Mater. Chem. A*, 2018, **6**, 17303–17306.

11 Q. Liu, X. Zhang, B. Zhang, Y. Luo, G. Cui, F. Xie and X. Sun, *Nanoscale*, 2018, **10**, 14386–14389.

12 J. Kong, A. Lim, C. Yoon, J. H. Jang, H. C. Ham, J. Han, S. Nam, D. Kim, Y.-E. Sung, J. Choi and H. S. Park, *ACS Sustainable Chem. Eng.*, 2017, **5**, 10986–10995.

13 D. Bao, Q. Zhang, F. Meng, H. Zhong, M. Shi, Y. Zhang, J. Yan, Q. Jiang and X. Zhang, *Adv. Mater.*, 2017, **29**, 1604799.

14 V. Kordali, G. Kyriacou and C. Lambrou, *Chem. Commun.*, 2000, **17**, 1673–1674.

15 L. Zhang, X. Ji, X. Ren, Y. Ma, X. Shi, Z. Tian, A. M. Asiri, L. Chen, B. Tang and X. Sun, *Adv. Mater.*, 2018, **30**, 1800191.

16 S. Chen, S. Perathoner, C. Ampelli, C. Mebrahtu, D. Su and G. Centi, *Angew. Chem.*, *Int. Ed.*, 2017, **56**, 2699–2703.

17 H. Huang, L. Xia, R. Cao, Z. Niu, H. Chen, Q. Liu, T. Li, X. Shi, A. M. Asiri and X. Sun, *Chem. Eur. J.*, 2018, **25**, 1914–1917.

18 C. Lv, C. Yan, G. Chen, Y. Ding, J. Sun and Y. Zhou, G. Yu, *Angew. Chem.*, *Int. Ed.*, 2018, **130**, 6181–6184.

19 Y. Liu, Y. Su, X. Quan, X. Fan, S. Chen, H. Yu, H. Zhao, Y. Zhang and J. Zhao, *ACS Catal.*, 2018, **8**, 1186–1191.

20 C. Lv, Y. Qian, C. Yan, Y. Ding, Y. Liu, G. Chen and G. Yu, *Angew. Chem., Int. Ed.*, 2018, **57**, 10246–10250.

21 Y. Zhang, W. Qiu, Y. Ma, Y. Luo, Z, Tian, G. Cui, F. Xie, L. Chen, T. Li and X. Sun, *ACS Catal.*, 2018, **8**, 8540–8544.